Terra Nova

doi: 10.1111/ter.12077

A middle–late Ediacaran volcano-sedimentary record from the eastern Arabian-Nubian shield

David Nettle,[1,7] Galen P. Halverson,[1,2] Grant M. Cox,[2] Alan S. Collins,[1] Mark Schmitz,[3] James Gehling,[4] Peter R. Johnson[5] and Khalid Kadi[6]

[1]*Tectonics, Resources and Exploration (TRaX), School of Earth and Environmental Sciences, University of Adelaide, Adelaide, SA 5005, Australia;* [2]*Department of Earth and Planetary Sciences/Geotop, McGill University, Montréal, H3A 0E8, Canada;* [3]*Department of Geosciences, Boise State University, Boise, ID 83725, USA;* [4]*South Australian Museum, North Terrace, Adelaide, SA 5005, Australia;* [5]*Consultant, 6016 SW Haines St., Portland, OR 97219, USA;* [6]*Saudi Geological Survey, P.O. Box 54141 Jiddah, 21514 Saudi Arabia;* [7]*Present address: Santos Ltd., 60 Flinders St, Adelaide, SA 5000, Australia*

ABSTRACT

The Ediacaran Jibalah Group comprises volcano-sedimentary successions that filled small fault-bound basins along the NW–SE-trending Najd fault system in the eastern Arabian-Nubian Shield. Like several other Jibalah basins, the Antaq basin contains exquisitely preserved sedimentary structures and felsic tuffs, and hence is an excellent candidate for calibrating late Ediacaran Earth history. Shallow-marine strata from the upper Jibalah Group (Muraykhah Formation) contain a diversity of load structures and intimately related textured organic (microbial) surfaces, along with a fragment of a structure closely resembling an Ediacaran frond fossil and a possible specimen of *Aspidella*. Interspersed carbonate beds through the Muraykhah Formation record a positive $\delta^{13}C$ shift from −6 to 0‰. U-Pb zircon geochronology indicates a maximum depositional age of ~570 Ma for the upper Jibalah Group, consistent with previous age estimates. Although this age overlaps with that of the upper Huqf Supergroup in nearby Oman, these sequences were deposited in contrasting tectonic settings on opposite sides of the final suture of the East African Orogen.

Terra Nova, 26, 120–129, 2014

Introduction

The Arabian-Nubian Shield (ANS) spans the north-east African and western Arabian plates (Fig. 1). It is a mosaic of accreted Neoproterozoic arcs, granitoid intrusions, syn-tectonic sedimentary basins, ophiolite slivers and older crustal fragments. It comprises the northernmost strand of the East African Orogen (EAO), where it was caught up between colliding fragments of eastern Gondwana and the Sahara metacraton during closure of the Mozambique Ocean (Pallister *et al*., 1988; Stern, 1994; Johnson and Woldehaimanot, 2003; Johnson *et al*., 2011, 2013). The ANS finished assembling close to the Precambrian–Cambrian boundary. Cryogenian and younger sedimentary basins are common across the ANS, but whereas the older basins are dominantly arc-related and allochthonous, most basins post-dating 650 Ma nonconformably overlie the amalgamated terranes (Johnson *et al*., 2011, 2013). Among the youngest and least deformed of these basins are over a dozen, small fault-bound basins that lie within the north-west-trending, sinistral Najd fault system in the northern third of the Arabian Shield (Fig. 1). These basins are filled mainly by mildly deformed and metamorphosed, terrestrial to shallow-marine successions of mixed siliciclastics, bimodal volcanics and carbonates, collectively known as the Jibalah Group (Delfour, 1970; Hadley, 1974; Al-Husseini, 2011). The Jibalah Group is roughly constrained to a middle–late Ediacaran age (Kusky and Matsah, 2003; Miller *et al*., 2008; Nicholson *et al*., 2008; Vickers-Rich *et al*., 2010, 2013; Al-Husseini, 2011); hence, it is coeval with at least part of the intensely studied and petroliferous Huqf Supergroup (Grantham *et al*., 1988) in Oman. The relative (present) proximity of the Jibalah basins and the Huqf basin, their comparable juvenile basement and similar ages have led some to argue that the Jibalah Group and Huqf Supergroup were deposited in a single, large basin post-dating the EAO and related to movement on the Najd faults (Loosveld *et al*., 1996; Le Guerroué *et al*., 2006a; Allen, 2007).

Previous work on the Jibalah Group has revealed possible Ediacaran fossils. Miller *et al*. (2008) reported *Beltanelloides*-like structures, putative burrows and a possible *Pteridinium* imprint, and Vickers-Rich *et al*. (2013) identified possible *Charnia*-like fronds, holdfasts and *Harniella* sp. traces fossils in the Dhaiqa Formation, in the north-western part of the shield. Vickers-Rich *et al*. (2010) also reported possible *Eoandromeda octiobrachiata* and *Nemiana* from the Jibalah Group. These provocative discoveries and available Ediacaran radiometric ages (Johnson *et al*., 2011) motivate closer investigations of the Jibalah basins (Johnson, 2006), which are a potentially important window into latest Precambrian biospheric change (Vickers-Rich *et al*., 2013). Here, we present additional putative Ediacaran fossil discoveries, along with sedimentological, geochronological and isotopic results from the Antaq basin, one of the larger and best exposed of the Jibalah

Correspondence: Dr Galen P. Halverson, Department of Earth & Planetary Sciences, McGill University, Montréal, QC H3A 2A7, Canada. Tel.: +1 514 398 4894; e-mail: galen.halverson@mcgill.ca

© 2013 John Wiley & Sons Ltd

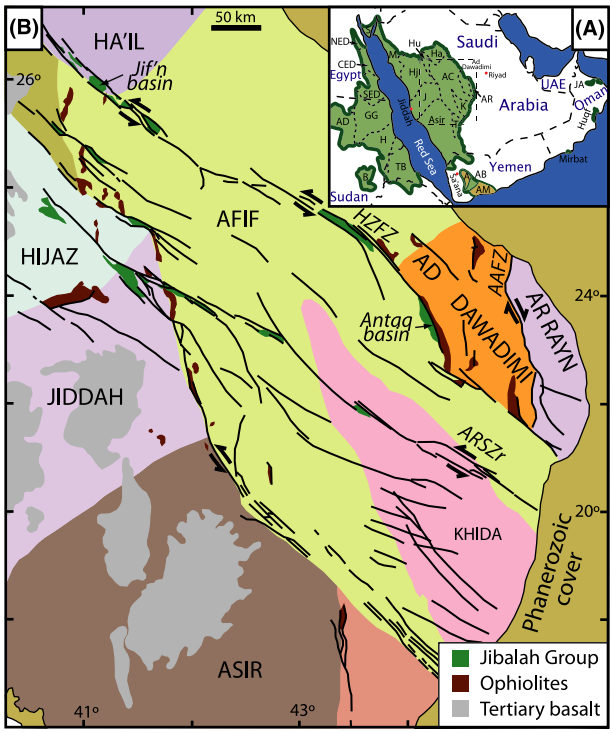

Fig. 1 (A) Location map showing the terranes of the composite Arabian-Nubian shield and other Proterozoic terranes of the Arabian Peninsula. TB: Tokar/Barka; B: Butana; H: Haya; GG: Gabgaba-Gebeit; AD: Atmur-Delgo; SED: South Eastern Desert; CED: Central Eastern Desert; NED: North Eastern Desert; S: Sinai; M: Midyan; Hj: Hijaz; Hu: Hulayfa; J: Jiddah; A: Abas; AB: Al Bayda; AM: Al Mahfid; T: Tathlith; K: Khida subterrane; AC: Afif composite terrane; AR: Ar Rayn; Ha: Ha'il; JA: Jebel Akhdar. (B) Map of the eastern Arabian Shield (with terranes shaded in different colours), showing location of the Antaq basin and other key Jibalah Group basins, along with ophiolites, which cluster along the terrane boundaries. HZFZ, Halaban-Zargat Fault Zone; AAFZ, Al Amar Fault Zone. ARSZr, Ar Rika Shear Zone.

Group basins (Fig. 1). These results confirm a middle–late Ediacaran age for the Jibalah Group, and highlight its potential to calibrate latest Precambrian Earth history.

Tectonic setting

The ANS began to form ~870 Ma ago during initial breakup of Rodinia, with the north–south accretion of island arcs and microcontinents. The orientation of accretion shifted to west–east with the onset of closure of the Mozambique Ocean at ca. 780–760 Ma (Johnson and Woldehaimanot, 2003). The youngest arc-affinity magmatism (*c.* 600 Ma; Doebrich *et al.*, 2007) occurred in the Ar Rayn terrane in the easternmost exposed ANS (Fig. 1). Whereas it has previously been postulated that Oman had accreted to the eastern ANS by *c.* 650 Ma and that the suture marking the closure of the Mozambique Ocean lies within the exposed eastern part of the shield (Stern, 1994; Allen, 2007), Cox *et al.* (2012) argued based on new age constraints from the Ad Dawadami terrane (Fig. 1) that closure occurred after ~620 Ma, with the final suture buried below Phanerozoic cover to the east. Consequently, Abu Mahara faulting in Oman, which generated *c.* 725–635 Ma rift basins that initiated deposition of the Huqf Supergroup (Loosveld *et al.*, 1996; Allen, 2007), appears to be unrelated to the Najd faults that reactivated and displaced terrane boundaries in the eastern ANS (Doebrich *et al.*, 2007).

The Najd fault system is a northwest trending, >200-km-wide suite of transpressional faults widely believed to have formed as the result of northward extension and lateral escape resulting from oblique collision of India with the ANS at the end of the EAO (Stern, 1994; Kusky and Matsah, 2003; Johnson *et al.*, 2011). The principle exposures of the Jibalah Group occur in isolated basins up to 20 by 100 km wide (Al-Husseini, 2011; Johnson *et al.*, 2011) along strands of the Najd fault system straddling the Afif terrane in the eastern ANS (Fig. 1). Whereas some authors have suggested that the present distribution of the Jibalah Group is the result of displacement of fragments of a larger master basin on the Najd faults (Al-Shanti, 1993; Nicholson *et al.*, 2008), most workers now regard the individual outcrops as distinct pull-apart or extensional basins related to early dextral displacement (Kusky and Matsah, 2003; Johnson *et al.*, 2011). The Antaq basin (8 by 45 km), originally mapped by Delfour (1982), is located on the eastern margin of the Afif composite terrane and bound to the east by the ophiolite-decorated Halaban-Zhargat Fault Zone (HZFZ; Fig. 2A). It comprises a nearly 2.4-km-thick panel of shallowly eastward-dipping strata, which, like most other occurrences of the Jibalah Group, has been folded by subsequent sinistral slip (Kusky and Matsah, 2003) on the Najd faults but is only minimally metamorphosed.

Stratigraphy

The Jibalah Group in the Antaq basin was previously subdivided into two formations: the lower Umm al Aisa formation, comprising a basal conglomerate and associated sandstone, and the Jifn formation, which makes up nearly the entire succession (Delfour, 1979). We apply different terminology based on the revised correlation of the Jibalah Group and nomenclature of Al-Husseini (2011), adopted from one of the earliest studies on these rocks (Hadley, 1974). Hence, the Jibalah Group in the Antaq basin is here subdivided into the Rubtayn, Badayi and Muraykhah formations (Fig. 2).

The ~1.8-km-thick Rubtayn Formation rests nonconformably on the Suwaj subterrane of the eastern Afif terrane (Fig. 2A). Suwaj basement comprises mainly *c.* 680 Ma granodiorite and tonalites (Stacey

© 2013 John Wiley & Sons Ltd

13653121, 2014, 2, Downloaded from https://onlinelibrary.wiley.com/doi/10.1111/ter.12077 by University Of The Western Cape, Wiley Online Library on [05/11/2024]. See the Terms and Conditions (https://onlinelibrary.wiley.com/terms-and-conditions) on Wiley Online Library for rules of use; OA articles are governed by the applicable Creative Commons License

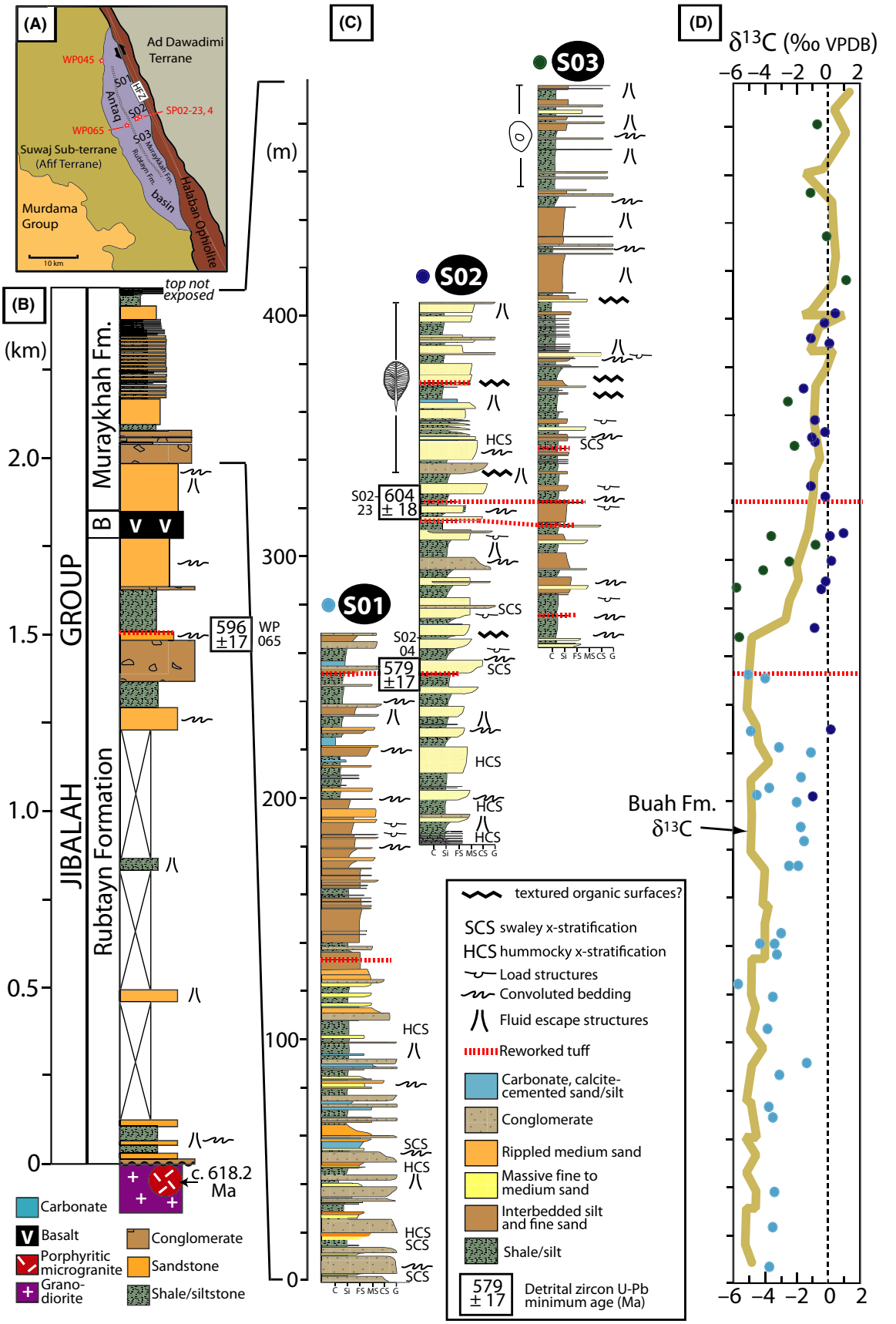

© 2013 John Wiley & Sons Ltd

13653121, 2014, 2, Downloaded from https://onlinelibrary.wiley.com/doi/10.1111/ter.12077 by University Of The Western Cape, Wiley Online Library on [05/11/2024]. See the Terms and Conditions (https://onlinelibrary.wiley.com/terms-and-conditions) on Wiley Online Library for rules of use; OA articles are governed by the applicable Creative Commons License

et al., 1984; Cole and Hedge, 1986), but much younger intrusive ages occur throughout the Afif terrane, including a suite of felsic dykes and microgranite plugs that intrude the thick Murdama Group to the west (Fig. 2A), where they yield U-Pb Sensitive High Resolution Ion MicroProbe (SHRIMP) ages of *c.* 610–600 Ma (Kennedy *et al.*, 2010, 2011). A similar microgranite occurs just below the contact with the Jibalah Group and has been dated at 618.17 ± 0.20 Ma (see below), providing a maximum age constraint on Jibalah deposition.

The base of the Rubtayn Formation (Fig. 2B) is a polymictic conglomerate, overlain by fine feldspathic and micaceous sandstone and siltstone with abundant carbonate concretions and m-scale fluid escape structures, as well as convoluted bedding and slump folds. Much of the middle Rubtayn Formation is poorly exposed in the alluvial plain west of Jabal Antaq, but where it does outcrop, it comprises sand and silt facies that resemble those in the lower part of the formation. The upper (intermittently exposed) 500 m of the Rubtayn Formation consists of siltstone, sandstone and a >200-m-thick polymictic, mostly massive conglomerate, interpreted as alluvial in origin. The lowermost dated tuff horizon (see below) occurs at the top of a medium-grained, feldspathic sandstone overlying the conglomerate (Fig. 2B). Fluid escape structures and convoluted bedding, although not as common as in the basal part of the formation, also occur in the upper siltstones and sandstones. The Rubtayn Formation is overlain by the poorly exposed, *c.* 100-m-thick volcanogenic Badayi Formation, which here consists of a series of discrete, subaerially extruded, alkali andesite–basalt flows (Delfour, 1979), in places separated by purple pyroclastic units.

The *c.* 400-m-thick Muraykhah Formation is spectacularly exposed in the N-trending Jabal Antaq (Fig. 3A), which trends slightly oblique to strike. The upper Muraykhah Formation is folded into an open, N-trending syncline that is truncated to the east by the Halaban-Zargat fault (Fig. 2A); hence, it lacks an upper stratigraphic contact. The lowermost Maraykhah Formation consists mainly of monotonous, medium-grained feldspathic sandstone with fluid escape structures and convoluted bedding (Fig. 3B), much like the Rubtayn Formation. It is overlain by intercalated, well-bedded to channelized pebble conglomerate, granular, feldspathic sandstone (Fig. 3C) and minor carbonate, arranged in crude, coarsening-upward cycles. Abundant tabular and trough cross-beds indicate palaeoflow to the south-east in a fluvial to delta plain environment. This interval transitions upward into a succession of mixed shale, siltstone, fine sandstone and carbonate arranged in striking, 5- to 20-m-thick, transgressive–regressive cycles (Fig. 3A, D). Where best developed, in section S02, the typical cycle has a sharp base and comprises convoluted shale or rippled siltstone, fining upward to a subtle maximum flooding surface (Fig 3D), then grading upward into fine to medium feldspathic sandstone with swaley cross-stratification, symmetric and asymmetric ripples, and tabular cross-bedding. Carbonates are common in the cycles and variably occur near the maximum flooding surface (Fig. 3D) or at the tops of cycles as carbonate-cemented fine sands or nodular cements.

Although much of the Jibalah Group in the Antaq basin was likely deposited in a non-marine environment, sedimentary structures in the middle–upper Muraykhah Formation imply deposition in a shallow, marginal marine setting. Symmetric ripples with consistent, unidirectional cross-lamination and reactivation surfaces, in some cases asymmetric in the opposite sense to the cross-lamination (Fig 3C), were likely formed by deposition from shoaling waves in a tidally influenced environment (Newton, 1968). WSW–ENE bimodal palaeocurrent directions (as measured in ripple cross-lamination and tabular cross-strata; Fig. 3E), along with rare herringbone cross-stratification, further support deposition in a shallow-marine, tidally influenced environment with a roughly NNW–SSE-trending coastline. The carbonates that occur at the maximum flooding surfaces of the cycles also imply a marine origin.

The Muraykhah Formation contains at least six conspicuous, reworked cream and tan-coloured volcanic tuffs (Fig. 3F), several of which are traceable over kilometres and the most prominent of which is 25 cm thick. These tuffs allow a reliable tephra correlation among the three measured sections (Fig 2C) along the best exposed, north-central part of the Jabal Antaq that shows that both the Muraykhah Formation as a whole and individual cycles fine and deepen to the south-east. Consequently, the deepest part of the basin is represented by the upper part of section S02 and section S03, where the cycles are predominantly sub-tidal shaley siltstone to fine sandstone.

Microbial textures and possible Ediacaran fossils

Peculiar, well-preserved, structures occur within rocks deposited in the shallow, sub-tidal setting of the middle–upper Muraykhah Formation. In some cases, these structures appear to be textured organic surfaces and in other cases exquisitely preserved load structures that resemble fragments of

Fig. 2 (A) Geological sketch map of the boundary between the Afif and Ad Dawadimi terranes showing the location of the Antaq basin. Closely spaced dashed lines show approximate location of the poorly exposed Badayi Formation. Red stars indicate locations of geochronology samples. (B) Generalized stratigraphic column of the Jibalah Group in the Antaq basin, with formation names based on the correlations proposed by Al-Husseini (2011) and radiometric ages for the Suwaj basement and youngest zircon in a tuff in the upper Rubtayn Formation. (C) Stratigraphic logs (S01–03) of the Muraykhah Formation in the Jabal Antaq [see (A) for locations of sections], along with correlation of traceable tuff horizons. Possible ranges of potential fossil locations are shown in sections S02 and S03. (D) Composite $\delta^{13}C$ column for Muraykhah Formation carbonates (see Table S1 for tabulated $\delta^{13}C$ and $\delta^{18}O$ data). Buah Formation (Oman) $\delta^{13}C$ profile from Fike *et al.* (2006) is shown for comparison.

© 2013 John Wiley & Sons Ltd

13653121, 2014, 2, Downloaded from https://onlinelibrary.wiley.com/doi/10.1111/ter.12077 by University Of The Western Cape, Wiley Online Library on [05/11/2024]. See the Terms and Conditions (https://onlinelibrary.wiley.com/terms-and-conditions) on Wiley Online Library for rules of use; OA articles are governed by the applicable Creative Commons License

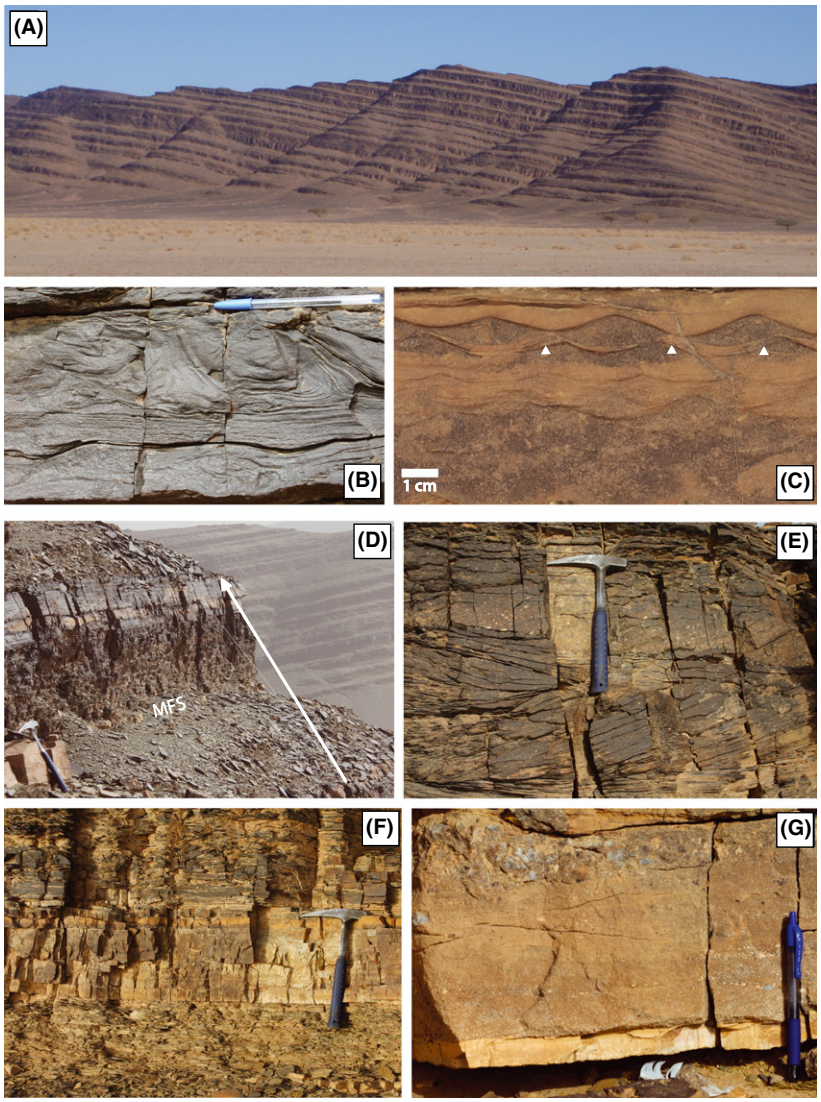

Fig. 3 (A) Panoramic view of the Jabal Antaq (facing east), showing well-developed cycles in the Muraykhah Formation (upper Jibalah Group). Note that the strike of bedding is oblique to the trend of the range, such that progressively younger strata are exposed to the south (right). (B) Convoluted bedding in fine sandstone in the Muraykhah Formation. Pen is 14.7-cm long, for scale (note the outcrop is covered in a patina of desert varnish). (C) Unidirectional (cross-lamination dipping to the left) symmetric ripples in fine sandstone. White triangles indicate reactivation (erosional) surfaces; the middle triangle points to rare cross-lamination dipping in the opposite direction. (D) A typical cycle in the Muraykhah Formation (arrow extends from maximum regression surface to maximum regressive surface). Pink–orange carbonate commonly occurs at the maximum flooding surface (MFS) of the cycles; here, it is almost 20 cm thick near the hammer (37 cm for scale). (E) Bimodal tangential, tabular cross-bedding, truncated above by a cross-bedded pebbly sandstone. (F) A typical felsic tuff within the Muraykhah Formation (hammer for scale). Note the sharp base and more transitional upper boundary of the tuff bed. (G) A thin (~2 cm thick) but laterally persistent tuff in the middle Muraykhah Formation with a sharp base and top, overlain by granular to pebbly sandstone.

frondose Ediacaran fossils. Textured organic surfaces (TOS) are a diverse subset of microbially induced sedimentary structures (Noffke *et al.*, 2002) that are the manifestation of the interaction among mats, their sandstone substrate and ambient hydrodynamic conditions (Gehling and Droser, 2009). TOS include well-studied 'elephant skin' (Gehling and Droser, 2009) and wrinkle textures, as well as a host of other structures (Bottjer and Hagadorn, 2007). TOS are commonly superimposed on other sedimentary structures, such as ripple marks, and many varieties reflect sedimentary loading that forms moulds and casts of microbial mats (Gehling, 1999; Gehling and Droser, 2009). A variety of different TOS morphologies occur in the middle–upper Muraykhah Formation including elephant skin, wrinkle, pucker and bulge structures (Fig. 4A–D, Fig S3; Nettle, 2009; Vickers-Rich *et al.*, 2010). These appear to define a continuum with more common load structures, which occur at multiple scales, with variably organized (regular, parallel ridges and troughs) and unorganized (irregularly shaped depressions and highs) forms. In some cases, loading clearly occurred on microbiallu bound surfaces (Fig. 4C). In many other cases, the load structures are not demonstrably biogenic, but their formation may have been made possible by the presence of biofilms separating what would otherwise be amalgamated sand beds (Bottjer and Hagadorn, 2007).

The two fossil specimens described here (see also Figure S4) were found within the range of abundant TOS (Fig. 2C) in the upper Muraykhah Formation; neither was found *in situ*, meaning their precise location within the sedimentary cycles has not been identified. The first specimen is from the upper part of section S02 (Fig. 2C) and resembles a fragment of an obovate-shaped *Charniodiscus* sp. (Ford, 1958; Jenkins and Gehling, 1978) petalomium preserved as a positive hyporelief cast in fine sand (Fig. 4F). Eighteen branches that terminate at an outer rim are observed, and some of these appear to preserve evidence of secondary modular elements. A second sample (Fig 4G) preserves three ~1-cm diameter, slightly prolate discs, each with a raised central boss. The three specimens, preserved in epirelief on the surface of a bed bearing a weakly developed elephant skin texture, resemble *Aspidella* sp. (Billings, 1872; Gehling *et al.*, 2000).

© 2013 John Wiley & Sons Ltd

13653121, 2014, 2, Downloaded from https://onlinelibrary.wiley.com/doi/10.1111/ter.12077 by University Of The Western Cape, Wiley Online Library on [05/11/2024]. See the Terms and Conditions (https://onlinelibrary.wiley.com/terms-and-conditions) on Wiley Online Library for rules of use; OA articles are governed by the applicable Creative Commons License

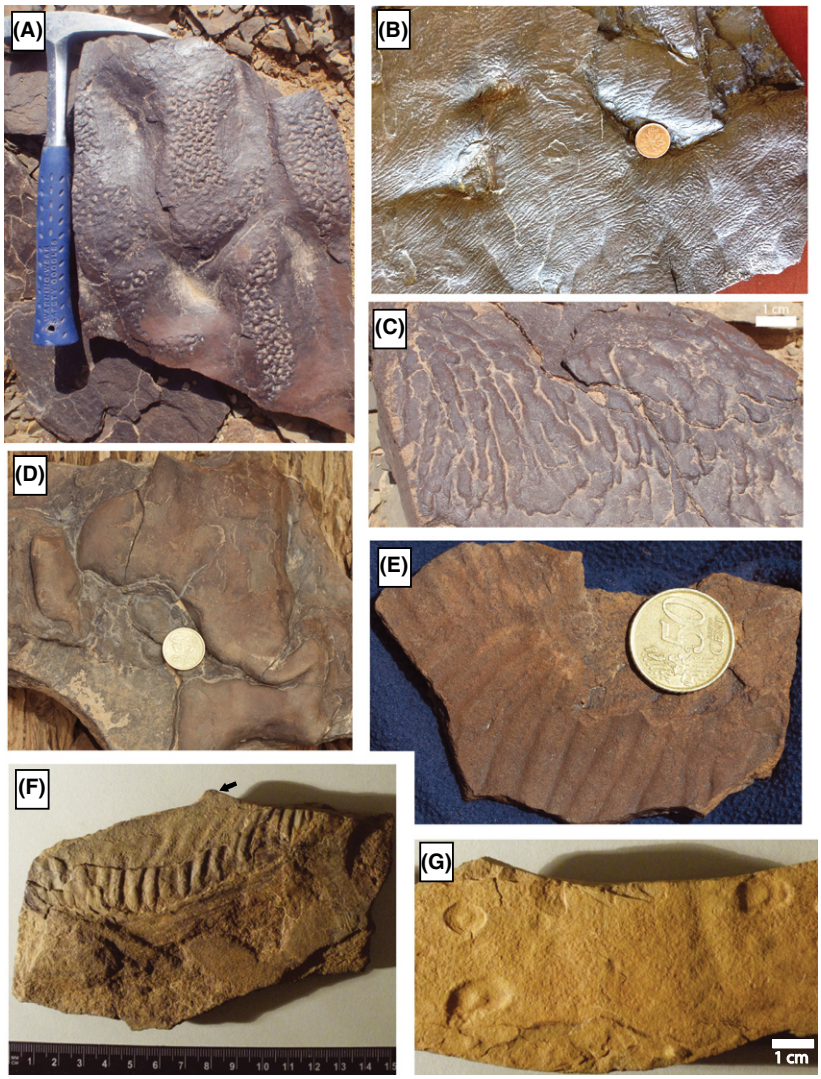

Fig. 4 Textured organic surfaces (TOS), load structures and dubiofossils in the Muraykhah Formation, Jabal Antaq. (A) Wrinkle structures preserved in ripple troughs on a bed sole. (B) Ropy wrinkle structure on load casts on the sole of a fine sandstone bed (with a patina of desert varnish) demonstrates the role of microbial mats as an interface between beds allowing for formation of load structures. Coin is 1.9 cm in diameter. (C) Non-transparent wrinkle structures (that is, the original microbial mat likely completely obscured the underlying substrate; Noffke *et al.*, 2002) with irregular moulds and casts on top of bed. White scale bar is 1 cm. (D) Irregular load casts on the sole of a bed where siltstone has loaded into underlying mudstone, with no evidence of biofilm or mat involvement. Coin for scale is 2.4 cm in diameter. (E) Organized load casts on sole of a fine sandstone bed resemble some wrinkle structures and superficially resemble a frond, but there is no evidence for involvement of a microbial mat. Loading may have been facilitated by a biofilm separating it from the underlying bed. Coin for scale is 2.6 cm in diameter. (F) A positive hyporelief cast (found in talus in the upper part of section S02) of what resembles a *Charniodiscus* frond (Nettle, 2009), with 18 apparent branches and what may be a stem (the knob on the top of the specimen, as shown by the arrow). Scale bar is in cm. SAM P48396. (G) Possible *Aspidella* sp. specimens preserved in epirelief on the sole of a sandstone bed bound by a microbial mat. Scale bar is 1 cm. SAM P48397. See Figure S4 for museum catalogue numbers and additional photos of specimens.

Carbon isotope stratigraphy

In several other Jibalah basins, the Muraykhah Formation is a dominantly carbonate unit (Delfour, 1970; Hadley, 1974; Kusky and Matsah, 2003; Johnson, 2006). At Jabal Antaq, carbonate is a minor but important component of the Muraykhah Formation, consisting of discrete <1-m-thick, yellow to brown, muddy to sandy limestone and dolostone beds. These carbonate beds occur both as nodules or caps at the tops of cycles and within finer-grained facies at the maximum flooding surface within the cycles (Fig. 3D). A total of 61 carbonate samples was collected from the three sections and measured for bulk carbon and oxygen isotope ratios (Fig. 2D; see Data S1 and Table S1). Whereas $\delta^{13}C$ values mostly cluster between −4 and 0‰, $\delta^{18}O$ is significantly more variable, ranging between −7 and +8‰ (Fig. S1). The highly ^{18}O-enriched values of some of the carbonates (at the tops of cycles) indicate that these rocks were deposited under evaporitic conditions, perhaps in an intermittently restricted basin. Nevertheless, $\delta^{13}C$ and $\delta^{18}O$ are uncorrelated, such that positive trends in $\delta^{18}O$ do not correspond to variations in $\delta^{13}C$ (see Table S1). The $\delta^{13}C$ data show significant scatter both stratigraphically and between sections, with no consistent correlation with facies; nevertheless, a rough trend towards higher values up-section is apparent.

The Antaq $\delta^{13}C$ values are distinctly lower than values obtained from the roughly equivalent Dhaiqa Formation (+1 to +5‰; Miller *et al.*, 2008) in the north-western part of the shield. This distinction implies that either one or both units do not record global seawater values, or that they are not precisely time correlative. The increase in $\delta^{13}C$ through the Muraykhah Formation is similar to the late Ediacaran $\delta^{13}C$ profile through the Buah Formation in nearby Oman (Fig. 2D), which records the end of the Shuram negative $\delta^{13}C$ anomaly (Le Guerroué *et al.*, 2006b; Grotzinger *et al.*, 2011). Although the age of the onset of the Shuram anomaly is controversial, its end is reasonably well constrained at *c.* 550 Ma

© 2013 John Wiley & Sons Ltd

13653121, 2014, 2, Downloaded from https://onlinelibrary.wiley.com/doi/10.1111/ter.12077 by University Of The Western Cape, Wiley Online Library on [05/11/2024]. See the Terms and Conditions (https://onlinelibrary.wiley.com/terms-and-conditions) on Wiley Online Library for rules of use; OA articles are governed by the applicable Creative Commons License

(Condon *et al.*, 2005), which is consistent with the age constraints for the Antaq basin, as discussed below. However, in light of the likelihood that the Muraykhah carbonates were deposited under restricted to non-marine conditions, we cannot confidently correlate the $\delta^{13}C$ profile with the end of the Shuram anomaly.

Geochronology

The only previously obtained direct constraints on the age of the Antaq Basin are *c.* 680 Ma U-Pb dates on granodiorites and tonalites of the Suwaj basement (Stacey *et al.*, 1984; Stoeser, 1986). However, approximate constraints are available from other Jibalah Group basins. In the Jifn basin, which lies to the northwest of the Antaq basin along the HZFZ (Fig. 1B), U-Pb zircon TIMS (Thermal Ionization Mass Spectrometry) ages of 624.9 ± 4.2 Ma and 576 ± 5.3 Ma have been obtained from rhyolite flows underlying the Jibalah Group and a felsite dyke that intrudes the upper Jibalah Group respectively (Kusky and Matsah, 2003). A single tuff in the Dhaiqa basin yielded a Laser Ablation-Inductively Coupled Plasma-Mass Spectrometry (LA-ICP-MS) concordia age of 569 ± 3 Ma (Vickers-Rich *et al.*, 2013), while various other Jibalah tuffs have yielded imprecise, minimum SHRIMP and LA-ICP-MS ages between 600 Ma and 560 Ma (Nicholson *et al.*, 2008; Vickers-Rich *et al.*, 2010).

We performed Chemical Abrasion-Thermal Ionisation Mass Spectrometry (CA-TIMS) U-Pb analyses on a porphyritic microgranite (sample WP045) in the basement to the Antaq basin and LA-ICP-MS U-Pb analyses on zircons separated from three tuffs within the Jibalah Group (Fig. 5; see Data S1 and Tables S3–S6). The microgranite yielded a weighted mean $^{206}Pb/^{238}U$ age ($n = 5$) of 618.17 ± 0.20 Ma. This age is slightly older and more precise than SHRIMP ages obtained on another porphyritic microgranite from the Afif terrane (*c.* 597 Ma; Kennedy *et al.*, 2010) and marginally younger than the 624.9 ± 4.2 age obtained on rhyolitic basement to the Jifn basin, which lies approximately 350 km NW of the Antaq basin along the HZFZ (Fig. 1B). Hence, this new age provides the tightest and most precise maximum age constraint available on the Jibalah Group in the Antaq basin and adds to the geochronological evidence for a significant felsic magmatic episode affecting the Afif terrane *c.* 620 Ma.

The stratigraphic locations of the three sampled tuffs are shown in Figure 2B, C. Sample WP065 was collected from the upper Rubtayn Formation and samples S02-04 and S02-23 from a pair of tuffs in the middle of the Muraykhah Formation in section S02 that can be traced continuously to section S03 (Fig. 2C). Although laminations and their occurrence within otherwise silty to sandy shallow-marine sediments suggest that the tuffs are partially reworked, their sharp bases (Fig. 3F, G) and petrographic analysis revealing abundant equant quartz, feldspar lathes, angular biotite, devitrified glass, and commonly broken, stubby, euhedral zircons suggest a pyroclastic origin. As is apparent in the spread of data in the U/Pb concordia and age spectra plots (Fig. 6), these populations are complicated by significant inheritance. Nevertheless, all three samples contain prominent Ediacaran age peaks (Fig. 6), which are clearly younger than reported ages from the underlying Cryogenian Afif terrane and the Ad Dawadimi and Ar Rayn terranes to the east (Stacey *et al.*, 1984; Doebrich *et al.*, 2007; Cox *et al.*, 2012). The youngest concordant 2σ $^{238}U/^{206}Pb$ ages from WP65, S02-04 and S02-23 are 596 ± 17, 579 ± 17 and 604 ± 18 Ma respectively. Although these results provide only an imprecise age constraint for the Jibalah Group, they nevertheless reinforce a middle–late Ediacaran age for the Muraykhah Formation. Palaeoproterozoic and late Mesoproterozoic zircons in samples WP065 and S02-04, respectively, strengthen isotopic evidence that the Afif composite terrane includes a component of older craton (Stoeser *et al.*, 2001; Stoeser and Frost, 2006; Johnson *et al.*, 2011).

Discussion and conclusions

The Ediacaran Antaq basin lies immediately west of the Halaban-Zhargat Fault Zone on the eastern margin of the Afif Terrane in central Saudi Arabia. Along with over a dozen similar, small, mildly deformed basins in the eastern Arabian shield, the Antaq basin presumably formed during an episode of transtensional deformation along the large Nadj Fault system in the latest stages of the East African orogeny, following stabilization of the Afif Terrane, but prior to final closure of the Mozambique ocean (Collins and Pisarevsky, 2005; Cox *et al.*, 2012). Much of the strata filling the basin are non-marine or of ambiguous (marine or non-marine) origin, but sedimentological and isotopic evidence suggest that the Mu-

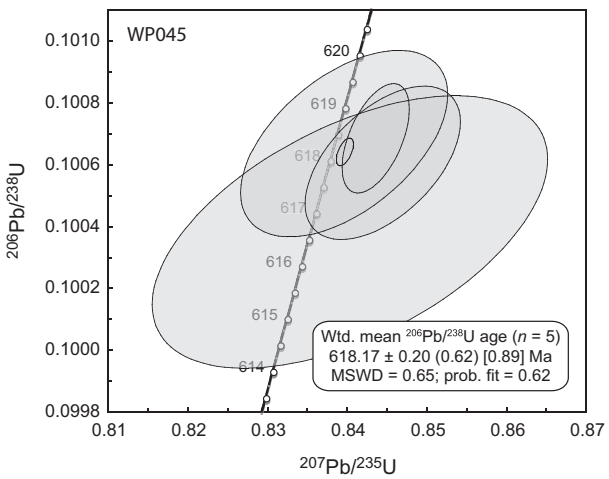

Fig. 5 Concordia diagram for CA-TIMS analyses of selected zircons from the WP045 porphyritic microgranite. High-U zircons were selected based on their lack of bright cores. Data-point error ellipses are 2σ.

© 2013 John Wiley & Sons Ltd

13653121, 2014, 2, Downloaded from https://onlinelibrary.wiley.com/doi/10.1111/ter.12077 by University Of The Western Cape, Wiley Online Library on [05/11/2024]. See the Terms and Conditions (https://onlinelibrary.wiley.com/terms-and-conditions) on Wiley Online Library for rules of use; OA articles are governed by the applicable Creative Commons License

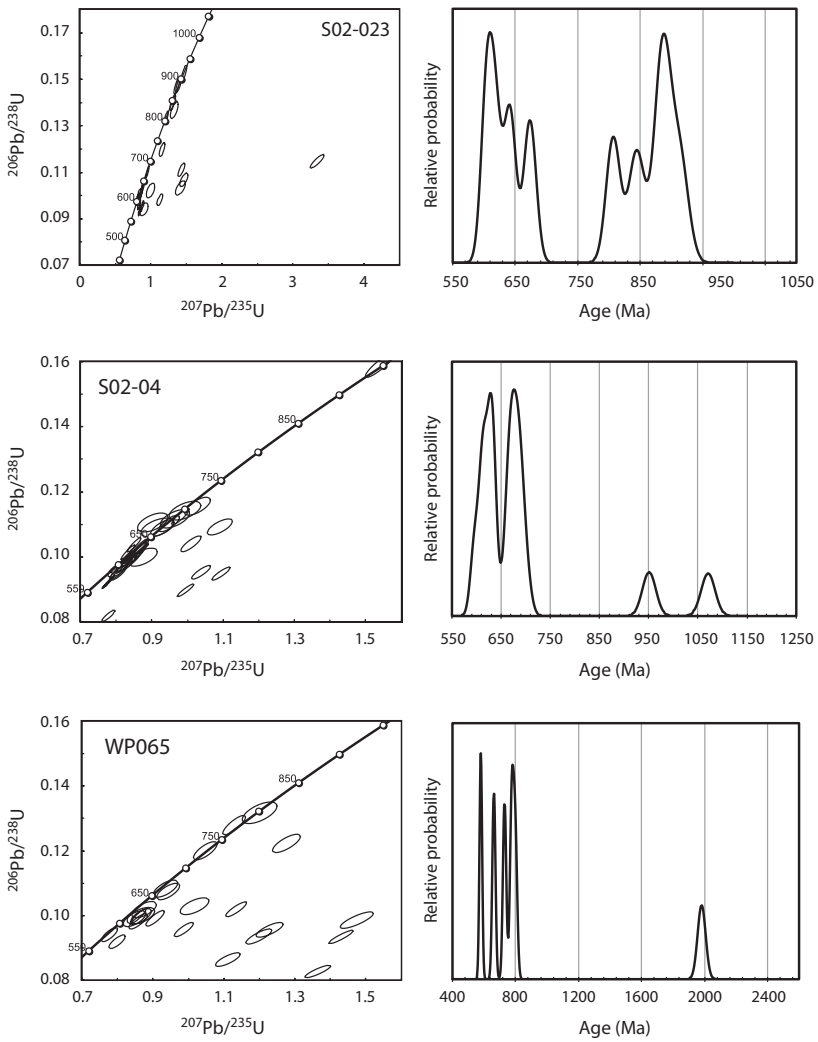

Fig. 6 Concordia diagrams and age spectra for the three tuff samples from the Jibalah Group. Data-point error ellipses are 2σ.

raykhah Formation in the Antaq basin records a transition to shallow-marine deposition. Hence, some of the Jibalah basins were open at least episodically to the western Mozambique Ocean. Available radiometric data, including CA-TIMS and LA-ICP-MS dates from the Jabal Antaq, confirm age constraints from elsewhere on the shield (see Johnson *et al.*, 2011 for a review), indicating that the Jibalah Group is middle to latest Ediacaran in age. However, some inconsistencies in U-Pb ages and carbon isotope data between basins present the possibility that the Jibalah Group is not everywhere time correlative. A degree of diachronism in the age of the Jibalah basins would not be unexpected insofar as they all formed in geographical isolation. Although the Jibalah Group tuffs have proven to be complex and difficult to date precisely, tighter age constraints on these basins should be possible and will be important to understand better their origin and duration.

The combination of a middle–late Ediacaran age (*c.* 580–560 Ma), inferred shallow intertidal to subtidal depositional setting of the middle–upper Muraykhah Formation, exceptional preservation of sedimentary structures, and evidence for microbial colonization of sand and silt surfaces combine to make the upper Jibalah Group highly prospective for Ediacaran fossils (Gehling, 1999). Putative Ediacaran fossils have been reported from other Jibalah basins. These include possible cross-cutting, looping and bifurcating structures resembling trace fossils and structures and impressions resembling *Pteridinium*, *Cyclomedusa, Aspidella* and *Charnia* in peritidal sediments of the Dhaiqa formation (Miller *et al.*, 2008; Vickers-Rich *et al.*, 2013). Possible *Beltanoides* and/or *Nemiana,* which may have an algal affinity, have also been reported from the Muraykhah formation in the Rubtayn basin (Vickers-Rich *et al.*, 2010). A fragment in float of what closely resembles a *Charniodiscus* frond (Fig. 4F) was found in the upper Muraykhah Formation in the Jabal Antaq. The *Aspidella*-like fossils (Fig. 4G) are complete, but also found in only one specimen, again in float. Individually, neither of these specimens constitutes robust evidence that Ediacaran fossils are preserved in the Jibalah Group. However, the increasing number and diversity of tantalizing specimens from the Jibalah basins that closely resemble known Ediacaran fossils, along with the unambiguous evidence that microbial mats stabilized the substrate in the shallow-marine realm of the Jibalah basins, make it likely that the Ediacaran biota populated the western Mozambique Ocean. Hence, Jibalah basins, with their abundant felsic tuffs, locally abundant carbonate, and exquisitely preserved sedimentary structures, hold great potential for further elucidating Ediacaran Earth history.

Acknowledgements

This study was supported by the Saudi Geological Survey, a National Geographic Research and Exploration grant, and an NSERC Discovery grant to GPH. This study was improved by a useful critique from an anonymous reviewer. This contribution is TRaX record #268.

References

Al-Husseini, M., 2011. Late Ediacaran to early Cambrian (Infracambrian) Jibalah Group of Saudi Arabia. *GeoArabia*, **16**, 69–90.

Allen, P., 2007. The Huqf Supergroup of Oman: basin development and context for Neoproterozoic glaciation. *Earth Sci. Rev.*, **84**, 139–185.

© 2013 John Wiley & Sons Ltd

13653121, 2014, 2, Downloaded from https://onlinelibrary.wiley.com/doi/10.1111/ter.12077 by University Of The Western Cape, Wiley Online Library on [05/11/2024]. See the Terms and Conditions (https://onlinelibrary.wiley.com/terms-and-conditions) on Wiley Online Library for rules of use; OA articles are governed by the applicable Creative Commons License

Al-Shanti, A.M.S., 1993. *The Geology of the Arabian Shield [in Arabic]*. Center for Scientific Publishing, King Abdlaziz University, Saudi Arabia.

Billings, E., 1872. Fossils in Huronian rocks. *Can. Nat. Quart. J. Science*, **6**, 478.

Bottjer, D. and Hagadorn, J.W., 2007. Mat growth features. In: *Atlas of Microbial Mat Features Preserved Within the Clastic Rock Record* (J. Scheiber, P. K. Bose, P. G. Eriksson, S. Banerjee, S. Sarkar, W. Altermann and O. Catuneao, eds), pp. 53–71. Elsevier, Amsterdam.

Cole, J.C. and Hedge, C.E., 1986. Geochronologic Investigation of Late Proterozoic Rocks in the Northeastern Shield of Saudi Arabia. Saudi Arabian Deputy Ministry of Mineral Resources, Jiddah, Saudi Arabia, USGS-TR-05-5, pp. 1–42.

Collins, A.S. and Pisarevsky, S.A., 2005. Amalgamating eastern Gondwana: the evolution of the Circum-India Orogens. *Earth Sci. Rev.*, **71**, 229–270.

Condon, D., Zhu, M., Bowring, S., Jin, Y., Wang, W. and Yang, A., 2005. From the Marinoan glaciation to the oldest bilaterians: U-Pb ages from the Doushantuo Formation, China. *Science*, **308**, 95–98.

Cox, G.M., Lewis, C.J., Cox, A.S., Halverson, G.P., Jourdan, F., Foden, J., Netle, D. and Kattan, F., 2012. Ediacaran terrane accretion within the Arabian-Nubian Shield. *Gondwana Res.*, **21**, 341–352.

Delfour, J., 1970. Le group de J'Balah, une nouvelle unité du Bouclier Arabe. *Bull. Bur. Rech. Géol. Min.* (ser. 2) **4**, 19–32.

Delfour, J., 1979. Geological Map of the of the Halaban quadrangle, Sheet 23G, Kingdom of Saudi Arabia. Saudi Arabian Directorate General of Mineral Resources, Jiddah, Saudi Arabia, GM 46, pp. 1–32

Doebrich, J.L., Al-Jehani, A.M., Siddiqui, A.A., Hayes, T.S., Wooden, J.L. and Johnson, P.R., 2007. Geology and metallogeny of the Ar Rayn terrane, eastern Arabian shield: evolution of a Neoproterozoic continental-margin during assembly of Gondwana within the East Africa orogen. *Precambrian Res.*, **158**, 17–50.

Fike, D.A., Grotzinger, J.P., Pratt, L.M. and Summons, R.E., 2006. Oxidation of the Ediacaran Ocean. *Nature*, **444**, 744–747.

Ford, T.D., 1958. Precambrian Fossils from Charnwood Forest. In: *Proc. Yorkshire Geol. Soc.*, **31**, 211–217.

Gehling, J.G., 1999. Microbial mats in Terminal Proterozoic siliciclastics: Ediacaran death masks. *Palaios*, **14**, 40–57.

Gehling, J.G. and Droser, M.L., 2009. Textured organic surfaces associated with the Ediacara biota in South Australia. *Earth Sci. Rev.*, **96**, 196–206.

Gehling, J.G., Narbonne, G.M. and Anderson, M.M., 2000. The first named Ediacaran body fossil, *Aspidella* terranovica. *Palaeontology*, **43**, 427–456.

Grantham, P.J., Lijmbach, G.W.M., Posthuma, J., Clarke, M.W.H. and Willink, R.J., 1988. Origin of crude oils in Oman. *J. Petrol. Geol.*, **11**, 61–80.

Grotzinger, J.P., Fike, D.A. and Fischer, W.W., 2011. Enigmatic origin of the largest-known carbon isotope excursion in Earth's history. *Nat. Geosci.*, **4**, 285–292.

Hadley, D.G., 1974. The taphrogeosynclinal Jubaylah Group in the Mashhad area, nortwestern Hijaz, Kingdom of Saudi Arabia. *Bull. Mineral Resour.* **10**, 18.

Jenkins, R.J.F and Gehling, J.G., 1978. A review of the frond-like fossils of the Ediacaran assemblage. *Rec. South Australian Mus. (Adelaide)* **17**, 347–359.

Johnson, P.R., 2006. Explanatory Notes to the Map of Proterozoic Geology of Western Saudi Arabia. Saudi Geological Survey Technical Report SGS-TR-2006-4, 62 p., Scale 1:1,500,000.

Johnson, P.R. and Woldehaimanot, B., 2003. Development of the Arabian-Nubian Shield: perspectives on accretion and deformation in the northern East African Orogen and the assembly of Gondwana. In: *Proterozoic East Gondwana: Supercontinental Assembly and Breakup* (B.F. Windley and S. Dasgupta, eds). *Geol. Soc. London Spec. Publ.*, **206**, 289–325.

Johnson, P.R., Andresen, A., Collins, A.S., Fowler, A.R., Fritz, H., Ghebreab, W., Kusky, T. and Stern, R.J., 2011. Late Cryogenian-Ediacaran history of the Arabian-Nubian Shield: a review of depositional, plutonic, structural, and tectonic events in the closing stages of the East African Orogen. *J. Afr. Earth Sci.*, **61**, 167–232.

Johnson, P.R., Halverson, G.P., Kusky, T., Stern, R.J. and Pease, V., 2013. Volcano-sedimentary basins in the Arabian-Nubian Shield: markers of repeated exhumation and denudation in a Neoproterozoic accretionary orogeny. *Geosciences*, **3**, 389–445.

Kennedy, A., Kozdroj, W., Kattan, F.H., Ziolkowskia-Kosdroj, M. and Johnson, P., 2010. SHRIMP Geochronology in the Arabian Shield (Midyan Terrane, Afif Terrane, Ad Dawadmi Terrane) and Nubian Shield (Central Eastern Desert Terrane), Part IV: Data Acquisition 2008. Saudi Geological Survey, Open-File Report SGS-OF-2010-10, 81p.

Kennedy, A., Kozdroj, W., Kadi, K., Ziolkowska-Kozdroj, M. and Johnson, P., 2011. SHRIMP Geochronology in the Arabian Shield (Midyan Terrane, Afif Terrane) and Nubian Shield (Central Eastern Desert Terrane), Part V: Data Acquisition 2009. Saudi Geological Survey, Open-File Report SGS-OF-2010-11. 80p.

Kusky, T.M. and Matsah, M.I., 2003. Neoproterozoic dextral faulting on the Najd Fault System, Saudi Arabia preceded sinistral faulting and escape tectonics related to closure Mozambique Ocean. In: *Proterozoic Eastern Gondwana: Supercontinent Assembly and Breakup* (M. Yoshida, B. F. Windley and S. Dasgupta, eds), *Geol. Soc. London Spec. Publ.*, **206**, 327–361.

Le Guerroué, E., Allen, P.A., Cozzi, A., Etienne, J.L. and Fanning, M., 2006a. 50 Myr recovery from the largest negative $\delta^{13}C$ excursion in the Ediacaran ocean. *Terra Nova*, **18**, 147–153.

Le Guerroué, E., Allen, P. and Cozzi, A., 2006b. Chemostratigraphic and sedimentological framework of the largest negative carbon isotopic excursion in Earth history: the Neoproterozoic Shuram Formation (Nafun Group, Oman). *Precambrian Res.*, **146**, 68–92.

Loosveld, R.J.H., Bell, A. and Terken, J.J.M., 1996. The tectonic evolution of interior Oman. *GeoArabia*, **1**, 28–51.

Miller, N., Johnson, P.R. and Stern, R.J., 2008. Marine versus non-marine environments for the Jibalah Group, NW Arabian Shield: a sedimentologic and geochemical survey and report of possible Metazoa in the Dhaiqa Formation. *Arab. J. Sci. Eng.*, **33**, 55–77.

Nicholson, P.G., Janjou, D., Fanning, C.M., Heaman, L.M., and Grotzinger, J.P., 2008. Deposition, age and Pan-African correlation of late Neoproterozoic outcrops in Saudi Arabia. In: *Proceedings of 8th Middle East Geoscience Conference and Exhibition*, Manama, Bahrain, pp. 2–5.

Nettle, D., 2009. *A sequence stratigraphic, geochronological and chemostratigraphic investigation of the Ediacaran Antaq basin, eastern Arabian Shield, Saudi Arabia*, MSc Thesis, University of Adelaide, Adelaide, Australia, pp. 1–84.

Newton, R.S., 1968. Internal structure of wave-formed ripple marks in the near-shore zone. *Sedimentology*, **11**, 275–292.

Noffke, N., Knoll, A.H. and Grotzinger, J.P., 2002. Sedimentary controls on the formation and preservation of microbial mats in siliciclastic deposits: a case study from the Upper Proterozoic

© 2013 John Wiley & Sons Ltd

13653121, 2014, 2, Downloaded from https://onlinelibrary.wiley.com/doi/10.1111/ter.12077 by University Of The Western Cape, Wiley Online Library on [05/11/2024]. See the Terms and Conditions (https://onlinelibrary.wiley.com/terms-and-conditions) on Wiley Online Library for rules of use; OA articles are governed by the applicable Creative Commons License

Nama Group, Namibia. *Palaios*, **17**, 533–544.
Pallister, J.S., Stacey, J.S., Fischer, L.B. and Premo, W.R., 1988. Precambrian ophiolites of Arabia: geological settings, U-Pb geochronology, Pb-isotope characteristics, and implications for continental accretion. *Precambrian Res.*, **38**, 1–54.
Stacey, J.S., Stoeser, D.B., Greenwood, W.R. and Fischer, L.B., 1984. U-Pb zircon geochronology and geological evolution of the Halaban-Al Amar region of the Eastern Arabian Shield, Kingdom of Saudi Arabia. *J. Geol. Soc.*, **141**, 1043–1055.
Stern, R.J., 1994. Arc assembly and continental collision in the Neoproterozoic East African Orogen: implications for the consolidation of Gondwanaland. *Annu. Rev. Earth Planet. Sci.*, **22**, 319–351.
Stoeser, D.B., 1986. Distribution and tectonic setting of plutonic rocks of the Arabian Shield. *J. Afr. Earth Sci.*, **4**, 21–46.
Stoeser, D.B. and Frost, C.D., 2006. Nd, Pb, Sr, and O isotopic characterization of Saudi Arabian Shield terranes. *Chem. Geol.*, **226**, 163–188.
Stoeser, D.B., Whitehourse, M. and Stacey, J., 2001. The Khida Terrane — Geology of the Paleoproterozoic rocks of the Muhayil area, eastern Arabian Shield, Saudi Arabia. *Gondwana Res.*, **4**, 192–194.
Vickers-Rich, P., Kozdroj, W., Kattan, F. H., Leonov, M., Ivantsov, A. and Johnson, P. R., 2010. Reconnaissance for an Ediacaran Fauna, Kingdom of Saudi Arabia. Saudi Geological Survey, Technical Report SGS-TR-2010-8, 42 p.
Vickers-Rich, P., Ivantsov, A., Kattan, F. H., Johnson, P.R., Al Qubsani, A., Kashghari, W., Leonov, M., Rich, T., Linnemann, U., Hofmann, M., Trusler, P., Smith, J., Yazedi, A., Rich, B., Al Garni, S.M., Shamari, A., Al Barakati, A. and Al Kaff, M., 2013. In Search of the Kingdom's Ediacarans: the First Genuine Metazoan (Macroscopic Body and Trace Fossils) from the Neoproterozoic Jibalah Group (Ediacaran) on the Arabian Shield. Saudi Geological Survey, Technical Report SGS-TR-2013-5, 21 p.

Received 17 June 2013; revised version accepted 4 October 2013

Supporting Information

Additional Supporting Information may be found in the online version of this article:

Data S1. Analytical Techniques

Table S1. $\delta^{13}C$ and $\delta^{18}O$ data for Murayhkah Formation carbonates, as shown Figures 2 and A1. *The 0-m datum for stratigraphic height is the base of the measured section.

Table S2. Location and description of samples for U-Pb geochronology.

Table S3. U-Pb data for WP045 zircons analysed by CA-TIMS (Figs 5 and A2).

Table S4. U-Pb data for WP065 zircons analysed by LA-ICP-MS (Fig. 6).

Table S5. U-Pb data for S02-04 zircons analysed by LA-ICP-MS (Fig. 6).

Table S6. U-Pb data for S02-023 zircons analysed by LA-ICP-MS (Fig. 6).

Figure S1. $\delta^{13}C$ vs. $\delta^{18}O$ cross-plot of carbonates from the Muraykhah Formation, revealing no distinct correlation and a wide spread in both $\delta^{13}C$ and $\delta^{18}O$ values, with notably ^{18}O-enriched values occurring in all three sections.

Figure S2. A. CL image of select zircons from sample WP045. Notice the bright cores and dark rims, which yield distinct trace element signatures (B–D). B-D. LA-ICP-MS measurements of cores and rims of zircons. Data plotting between the fields of the cores and rims are interpreted to reflect mixed spots. E. Age spectra for the WP045 zircons analysed by LA-ICP-MS. The youngest zircons, shown in green, yield a weighted mean age of 619.1 ± 4.6 Ma ($n = 10$), which is identical within error to the CA-TIMS age presented in Figure 6.

Figure S3. Additional specimens of possible textured organic surfaced, catalogued at the South Australian Museum. (A) SAM P47938. (B) SAM P47939. (C) SAM P47940.

Figure S4. Two catalogued putative Ediacaran fossil specimens. (A) SAM P47936. (B) SAM P47937.

© 2013 John Wiley & Sons Ltd

13653121, 2014, 2, Downloaded from https://onlinelibrary.wiley.com/doi/10.1111/ter.12077 by University Of The Western Cape, Wiley Online Library on [05/11/2024]. See the Terms and Conditions (https://onlinelibrary.wiley.com/terms-and-conditions) on Wiley Online Library for rules of use; OA articles are governed by the applicable Creative Commons License